OPEN ACCESS
Journal of Innovative Optical Health Sciences
Vol. 15, No. 6 (2022) 2240010 (15 pages)

DOI: 10.1142/S1793545822400107

World Scientific
www.worldscientific.com

Photoinactivation of *Escherichia coli* using five photosensitizers and the same number of photons

Daniel Ortega-Zambrano, Denisse Fuentes-López and Hilda Mercado-Uribe*
CINVESTAV-Monterrey, Parque PIIT,
Autopista al Aeropuerto km. 9.5,
Apodaca, NL 66600, México
**hmercado@cinvestav.mx*

Received 7 June 2022
Revised 8 August 2022
Accepted 9 August 2022
Published 14 September 2022

Bacterial resistance is today a matter of great medical concern, so it is urgent to investigate alternatives to alleviate it. Photodynamic inactivation (PDI) is a method that has been endorsed to inactivate different pathogens, including bacteria, fungi and viruses. PDI is achieved by using a photosensitizer (PS) molecule which generates reactive oxygen species under visible or UV radiation. We use visible light and UV-A radiation to excite four commercial PSs (methylene blue, rose bengal, riboflavin and curcumin), and nanoparticles synthesized in our laboratory. Despite these PSs having been thoroughly studied in the past by other research groups, in order to compare their effects in an appropriate way, we matched the number of photons they absorb. We found that methylene blue leads to the major inactivation of *Escherichia coli*. Furthermore, we evaluated the production of singlet oxygen and hydroxyl radicals in the photoinactivation process.

Keywords: Photodynamic inactivation; *E. coli*; ROS; photons.

1. Introduction

Despite the initial success of antibiotics, the resistance that bacteria develop against them is a serious alarm worldwide. There is a particular group of superbugs coined by the World Health Organization (WHO) as "ESKAPE", currently under special attention. These pathogens (*Enterococcus faecium*, *Staphylococcus aureus*, *Klebsiella pneumoniae*, *Acinetobacter baumannii*, *Pseudomonas aeruginosa* and *Enterobacter spp.*) are responsible of many nosocomial diseases that evade the antimicrobial action.[1–4] Four of them are Gram-negative bacteria. A social factor contributing to the development of bacterial resistance is the unsuitable and overindulgence prescription of antibiotics, as well as a common interruption of the treatments by patients.[1] It represents a considerable social and economic burden for the governments.

*Corresponding author.

In the past century, antibiotics were obtained from natural sources, like fungus and bacteria. Nowadays, such drugs are developed according to the key–lock principle, that is, from the identification of a specific site or molecule, called target, that is crucial for the microorganism.[5] Paradoxically, this is the main reason microorganisms develop resistance. Once an antibiotic is supplied, and because the replication speed of bacteria is high, a mutation may take place helping bacteria to survive. The resistance prevails in the cell population. In some cases, enzymes that promote the action of drugs may lose their activity, and enzymes that block it, like β-lactamases, can be produced in the cell.[6]

In 2018, the WHO made an urgent call to work on the development of new strategies against multidrug resistant and extensively in Gram-negative bacteria.[7] The problem, in general, has been approached from three different angles: introducing variations to the existing antibiotics, developing new drugs, and focusing on complementary therapies. A recent review analyzed and classified 407 antibacterial projects that are in the preclinical phase (before experiments with humans).[8] The authors emphasize that around 45% of these investigations employ small molecules (< 1 kDa) and one new target. Other works are addressed to enhance the effect of antibiotics, vaccines, or phages against pathogens. Efforts are mainly focused on Gram-negative organisms, whose notable resistance is due to an outer membrane that does not exist in Gram-positive bacteria. Such layer is mainly made up of lipoproteins, lipopolysaccharides (LPSs) and phospholipids (PLs). This envelop is a "barrier", so going against internal targets is an arduous task.[9–12] Even more worrying is that none of the new antibiotics have improved their response against such bacteria, therefore, there is a risk that resistant microorganisms may emerge.

We would like to remark that not only antibiotics generate resistance; antiseptics and biocides such as triclosan, benzalkonium chloride and chlorhexidine, as well as nanoparticles of silver also do.[13–15] They do not act on specific targets, bacteria employ defence mechanisms to expel these substances, for instance, by the action of drug efflux pumps.

Although photodynamic inactivation (PDI) has been employed since the last century, the interest arises again as a promising alternative treatment to antibiotic resistance. PDI has demonstrated to be not only an efficient method in the eradication of some pathogens, but in the suppression of the resistance development due to its nonselective action.[6] It is a noninvasive method based on the modification of the properties and function of biomolecules in pathogens by reactive oxygen species (ROS), generated indirectly by a nontoxic molecule (photosensitizer (PS)).[16–18] Initially, the PS molecule is in its ground state or minimum energy called singlet state (S0), where the two external electrons are paired (the spin quantum numbers are anti parallels). Once the PS is excited with a suitable wavelength, one of the electrons goes up to a more energetic state, called singlet excited state (S1), which is very unstable with a short half-life (in the order of nanoseconds). The PS eventually loses the excess of energy and gradually decays to the ground state by two mechanisms: fluorescence (with light emission) and internal conversion (with heat production). A third decaying mechanism is through intersystem crossing, where the PS results in a triplet state (T1). This is an excited state, more stable (half-life of microseconds) than the singlet state, due to the fact one of the external electrons flips the spin. T1 decays to S0 by two pathways: the most complex, the Type 1 process, involves redox reactions that lead to the formation of ROS, mainly, superoxide anion ($O^{\bullet -}$), hydrogen peroxide (H_2O_2) and hydroxyl radical ($HO^{\bullet}$). In particular, superoxide anion is nonbiologically reactive; however, it is a cascade trigger of other ROS when it is protonated, becoming in one biologically reactive radical.[16,17,19] In the Type II process, the PS transfers energy directly to the molecular oxygen ($^3O_2$), that is in a triplet state. Such process, faster than Type I, gives rise to a new molecule, more energized and highly reactive known as singlet oxygen ($^1O_2$). It is considered the most toxic species generated in PDI. Precisely because ($^1O_2$) it is extremely reactive, it has a short lifetime ($< 4\,\mu$s) and a short distance of action (≈ 150 nm).[16] The proportion of Types I and II processes depends on the PS, and they can occur individually or simultaneously.[3] Once the PS releases the absorbed energy, it can be excited again to generate new ROS. They may interact, mainly by oxidative processes, with different molecules or cellular structures and provoke direct and indirect effects in such components, or in the surrounding environment because of the oxidation products. One of the most critical direct damages is lipid peroxidation, that not only affects the membrane. Such

disturbance eventually leads to crucial biological injuries in the cell, and inactivation in pathogenic microbes.[16–18] The outcome of PDI depends on the chemical structure of the PS, as well as in their concentrations and molecular oxygen in the medium, wavelength of light, fluence rate and number of absorbed photons.[17]

The main features of the ideal antimicrobial PS are well known: nontoxicity in dark conditions, efficiency to generate ROS, selectivity from microbial over the host mammalian cells, and significant cationic charges.[9] In this context, several synthetic and natural dyes have been studied.[9,16–18]

PDI in Gram-negative bacteria is usually carried out with a cationic PS or combining either the PS with a divalent cation or a chelant ligand (a sequester of metal ions). In the first case $CaCl_2$ or $MgCl_2$ are used. Ethylenediaminetetraacetic acid (EDTA) can be employed as a chelant agent, which binds to charged molecules and removes divalent cations, resulting in the thermodynamic destabilization and disruption of the outer membrane. In fact, it has been widely reported that a pre-treatment with EDTA causes the loss up around 65% of LPS of *Escherichia coli* outer membrane and the facility of PS internalization.[4,10,11,20]

Biological effectiveness of different PS is commonly evaluated by matching the energy doses and comparing the response in the same cell.[3,21] Considering that every PS has a unique and a preponderant absorption, it has been recently suggested.[22] that the correct way to do such a comparison is by matching the number of absorbed photons per second (Ap/s) in each PS (instead of energy doses), obeying the following equation:

$$\mathrm{Ap/s} = \sum_{\lambda} (1 - 10^{-\varepsilon(\lambda)\cdot c_0 \cdot d}) \cdot P_{\mathrm{em}}(\lambda) \cdot \frac{\lambda}{c \cdot h}, \quad (1)$$

where λ is the wavelength of the light source, $\varepsilon(\lambda)$ the molar extinction coefficient at a given wavelength, c_0 the concentration of the PS (μM), d the thickness of the solution, P_{em} the spectral radiant power by the light sources, c the velocity of light and h the Planck constant.

Since, as far as we know, this important consideration has been applied only in few cases,[22–26] here we study the inactivation of *E. coli* cultures using five sensitizers: methylene blue (MB), rose bengal (RB), curcumin (C), riboflavin (R) and nanoparticles of pheomelanin (P) recently synthesized by us. P is a type of melanin (a yellow to reddish-brown

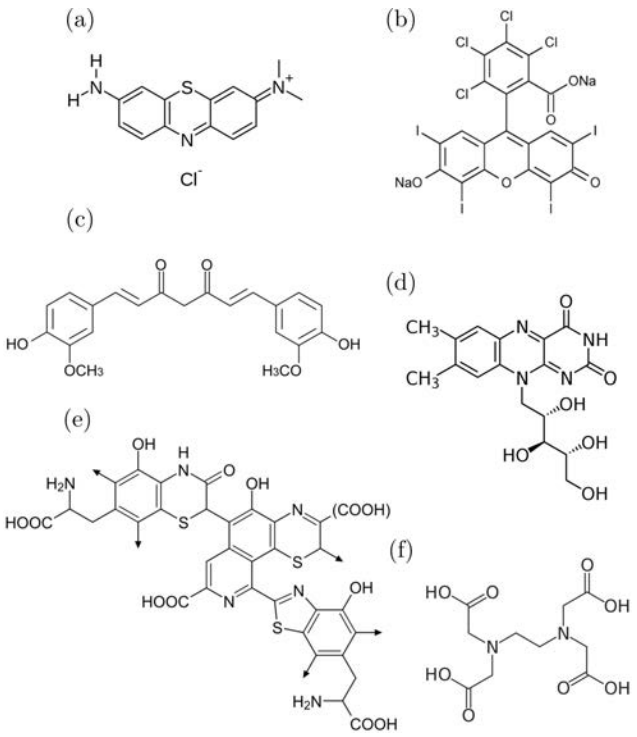

Fig. 1. Chemical structures of the PSs and chelant agent used in this study: (a) MB, (b) RB, (c) C, (d) R, (e) P (synthesized in the laboratory) and (f) EDTA.

pigment) soluble in alkali and it contains nitrogen as a characteristic feature. Studies using P are scarce, mainly because it is not commercially available and hard extraction in the laboratory is the only via to obtain it. We carried out the synthesis of this molecule from dopaquinone, which is formed by the oxidation of L-tyrosine and addition of L-cysteine.[27] The chemical structures of such PS are shown in Fig. 1.

2. Materials and Methods

2.1. *Sample preparation for photoinactivation*

The bacteria strain used in this work was *E. coli* K-12-MG-1655. Optical density of 0.4 (measured by Multiskan GO, Thermo Scientific), which corresponds to the exponential growth (see Fig. 2), was used for the experiments. Such density is equivalent to 2×10^8 colony forming units (CFU)/mL, according to the growth kinetics measurements. Four serial dilutions were made, the first by pouring 200 μL of the saturated bacterial solution into

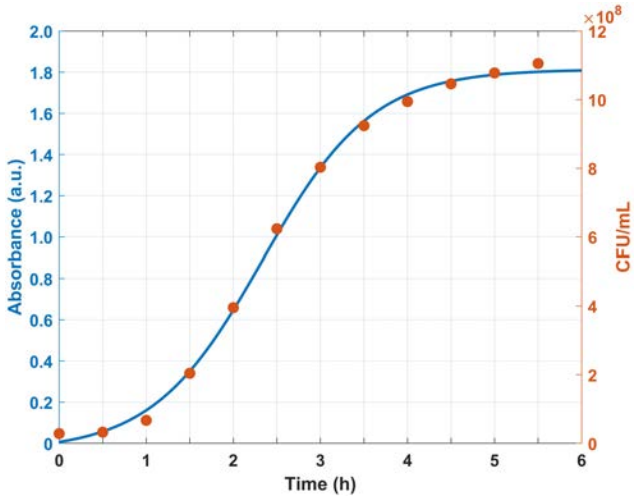

Fig. 2. *E. coli* growth curve in LB medium. The bacterial suspension was poured in a flask containing 200 mL of LB medium, and left for incubation, at 37°C and 130 rpm. The measurements were carried out in a polystyrene cuvette and the absorbance was recorded each 30 min for 5 h and half. The experiment was performed by triplicate. Brown circles represent the average and blue line the fit of the sigmoidal curve using a logistic function ($N_0 = -0.03794$, $N_{\text{asymp}} = 1.814$, $k = 1.589$, $t_c = 2.335$).[28] The confidence interval is 95% and the correlation coefficient is $r^2 = 0.9985$ (the errors are around 6%, smaller than the symbols). The solid cultures were performed in agar LB using the pour plate method to obtain CFUs.

20 mL of the LB broth stock solution. Next, we made three successive dilutions consisting of mixing 10 mL of the suspension bacteria and 10 mL of Luria Bertani (LB) broth. The suspensions were centrifuged at 4000 rpm for 4 min, washed and resuspended in 10 mM phosphate-buffered saline (PBS) and centrifuged again three times. To obtain the same rate of photon absorption for every PS, the concentrations were adjusted considering the PS and power of the source.[3] We show in Fig. 3 the rate of absorbed photons as a function of concentration for the PS exposed to the appropriate wavelength. C exhibits the most rapid absorption in photons for small variations in its concentration. P has a slow response as its concentration changes. According to these results, we considered that a best match for all PS is around 8.5×10^{15} absorbed photons. Therefore, the concentrations used were: 12.5 μg/mL (39.1 μM) for MB, 13.2 μg/mL (13 μM) for RB, 3.1 μg/mL (9.77 μM) for C, 54.5 μg/mL (145 μM) for R and 82.3 μg/mL for P. All of them were purchased from Sigma-Aldrich (MB: 61-73-4, RB: 632-69-9, C: 458-37-7 and R: 83-88-5, respectively), except P, which was synthesized in our laboratory. We evaluated the PS effect with and without the chelant agent (EDTA). In the first case, we had three control samples: (1) 100 μL of bacterial suspension with 900 μL of PBS solution, (2) 100 μL of bacterial suspension with 900 μL of EDTA solution in PBS buffer and (3) 100 μL of bacterial suspension with 900 μL of EDTA and PS solution in PBS buffer. In the second case, we had two control samples: (1) 100 μL of bacterial suspension with 900 μL of PBS solution, (2) 100 μL of bacterial suspension with 900 μL of PS solution in PBS. The dilutions were made by a factor of 10 respect to the stock solution. Only C was dissolved in ethanol (10%). 200 μL of each bacterial suspension were sown in a 96-well microplate, protected from light with aluminum foil and incubated for 30 min in these dark conditions at room temperature.

2.2. *Photodynamic inactivation*

Bacteria cultures were first exposed to red, green, blue and UV-A radiation for 60 min control experiments before the photoinactivation, which consisted in exposing the cells to the corresponding wavelength of maxima absorption of every PS: 660 nm for MB, 515 nm for RB, 450 nm for C and 375 nm for R and P. Control and experiments

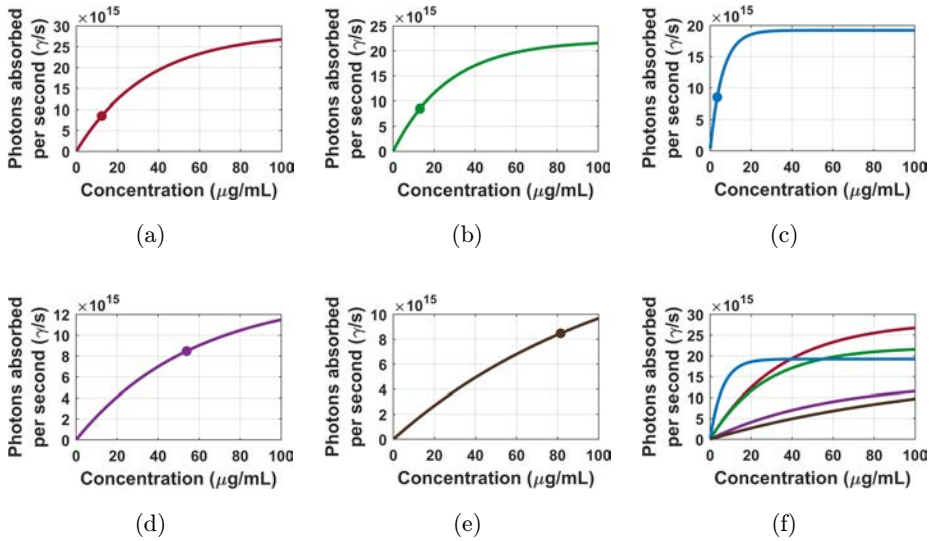

Fig. 3. The rate of absorbed photons (γ/s) by PS exposed to the appropriate wavelength as a function of concentration (μg/mL): (a) MB (12.5 μg/mL) at 660 nm, (b) RB (13.2 μg/mL) at 515 nm, (c) C (3.1 μg/mL) at 450 nm, (d) R (54.5 μg/mL) at 375 nm, (e) P (82.3 μg/mL) at 375 nm, (f) all the PS. The same rate of photon absorption for all PS, 8.5×10^{15} (indicated by the point) was adjusted considering the characteristics of PS and spectral radiant power of the corresponding light source.

samples were exposed at 95.27 J cm^{-2}. We would like to note that in order to calculate this dose we took into account the reflection of the laser on the bottom of culture microplate. Such contribution was around 6%.

Figure 4 shows the absorption spectra of every PS and spectral radiant power of the light sources used as a function of wavelength. Table 1 shows the main properties of such PSs (wavelength of maximum absorption, extinction coefficient and

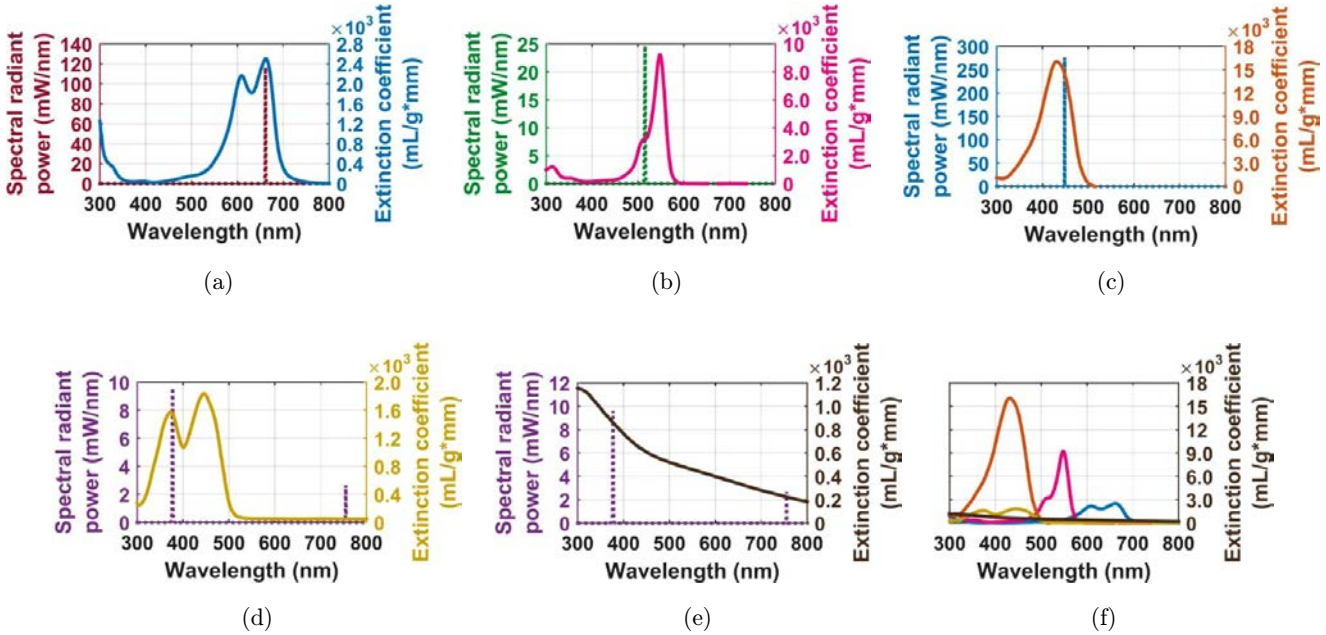

Fig. 4. The absorption spectra of PS (continuous line) and spectral radiant power of the light sources (dotted line) as a function of wavelength. Four commercial PS and one synthesized in the laboratory were exposed to radiation: (a) MB (660 nm), (b) RB (515 nm), (c) C (450 nm), (d) R (375 nm) and (e) P (375 nm). (f) The absorption spectra of all PS. The spectral width (at full width at half maximum) for each source is: 0.940 nm for the red laser (660 nm), 1.669 nm for the green (515 nm), 0.310 nm for the blue (450 nm) and 1.242 nm for the UV-A source (375 nm). Note that the widths are so small that the spectra look like vertical lines.

Table 1. Main properties of the PSs.

PS	λ (nm)	ε (mL g^{-1}mm^{-1})	Φ_Δ
MB	660	2487	0.5, 0.6, 0.22[a]
RB	515	3218	0.7, 0.76[a]
C	450	14,111	0.10, 0.05, 0.11[b]
R	375	1569	0.5, 0.59[c]
P	375	870	—

Notes: [a] References 29 and 30.
[b] References 29, 31 and 32.
[c] References 29 and 33.

quantum efficiency). For irradiations of MB, RB and C, we used laser diodes (300 mW RGB combined white a laser module mini stage lighting, Laserland); whereas R and P were excited by an UV-A laser (Excelsior, Spectra-Physics) with a main component at 375 nm. All the exposures were made at 16 mW. A circular neutral density filter (CVND15-B60C, Opto Science Inc.) was used to maintain the same incident radiation power (8 mW) independently of the emission source. Power was measured with a handheld-optical meter (1918-R, Newport) and the thickness of the solution (d) was 5 mm.

Figure 5 exhibits the main section of the experimental setup. The exposure time in these experiments was 60 min, corresponding to 95.27 J cm^{-2}. The irradiance value in the culture well was 26.45 mW cm^{-2}. Every experiment was performed by triplicate.

2.3. *CFU assays after photoinactivation*

In order to quantify the inactivation efficiency of the *E. coli* bacteria exposed to UV–visible radiation, we looked at the response of the different samples. 100 μL of every bacterial suspension were mixed with 900 μL of PBS buffer. Next, four serial dilutions were made. The resulting suspensions had a dilution factor between 10^{-2} and 10^{-5}. For every sample an aliquot of 100 μL was extracted and poured in a Petri dish with agar LB. This suspension was homogenized by shaking. Each solution was plated in triplicate and the number of colonies formed (CFU) was counted after 24–48 h of incubation at 37°C.

2.4. *Statistical analysis*

The results of the photoinactivation measurements are shown as medians including 25% and 75% quartiles. Statistical analysis was performed with the SPSS Software MATLAB 2021 from the values of at least three independent experiments, each one made in triplicate. The photoinactivation is reported as medians on or below the continuous and dashed lines indicating CFU diminutions of ≥ 3 $\log_{10}$ and ≥ 5 $\log_{10}$ steps, respectively, compared to the control (PBS).

2.5. *ROS detection by fluorescence*

In order to detect some of the ROS generated in the photoinactivation process, we used Singlet Oxygen

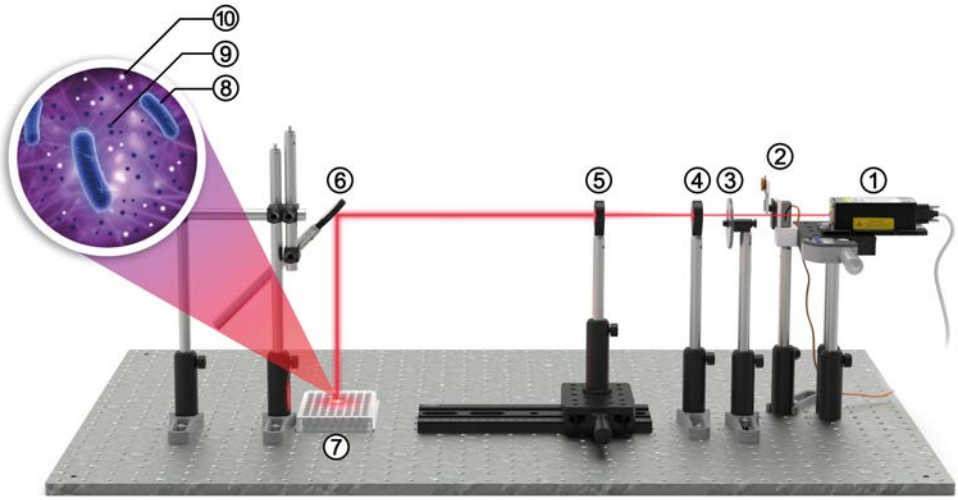

Fig. 5. The main section of the experimental setup used for photoinactivation of *E. coli* cultures: (1) laser, (2) shutter, (3) neutral density filter, (4) divergent lent, (5) convergent lent, (6) mirror, (7) transparent culture microplate (in the image shown white), (8) *E. coli* bacteria, (9) PS molecules and (10) chelant agent EDTA. The operation of this setup was done by a LabVIEW program.

Sensor Green, SOSG (Invitrogen, OR, USA) and hydroxyphenyl fluorescein, HPF (Invitrogen, OR, USA). Both are probe molecules highly sensitive and specific exhibiting a fluorescent signal when ROS are activated. SOSG reacts with $^1O_2$ resulting in SOSG endoperoxides (SOSG-EP), which emit green fluorescence with a maximum excitation and emission around 504 nm and 525 nm, respectively.[27] We prepared a stock solution of SOSG (40 μM) in methanol and water. We mixed one part of this solution with nine parts of PS in order to obtain the following final concentrations: 5.7 μg/mL for MB, 5.8 μg/mL for RB, 1.5 μg/mL for C, 21 μg/mL for R and 33.7 μg/mL for P. On the other hand, HPF is very sensitive to hydroxyl radical ($^{\cdot}$OH) and peroxynitrite anion ($ONOO^-$) exhibiting a green fluorescence upon oxidation, with a peak around 515 nm.[27] We also prepared stocks solutions of HPF (4 μM) and PS using the same proportions employed for SOSG, obtaining the same concentrations, except for the case of R (2.1 μg/mL), due to the saturation of the equipment. Fluorescence spectra of the samples contained in polystyrene cuvettes were acquired every 30 min with a FluoroMax-4 spectrofluorometer (HORIBA Jobin Yvon). SOSG was excited at 525 nm and SOSG-EP recorded between 400 nm and 800 nm. The excitation of HPF was at 490 nm and the fluorescence registered around 515 nm. The excitation and emission slits were set to 5 nm at room temperature. SOSG and HPF suspensions contained in a polystyrene cuvette were irradiated using an UVA laser (Excelsior 375 Spectra-Physics) for the case of R and P and a laser diode (300 mW Laserland RGB laser module RGB laser module) for the rest of PS. In all cases the incident radiant power was 8 mW (26.45 mW cm^{-2}).

2.6. *Singlet oxygen detection by an optical setup*

It is well known that the signal of $^1O_2$ is unique, with an emission at approximately 1275 nm, depending on the solvent. However, its detection is a real challenge due to its very short lifetime (10–300 ns in a cell), low emission probability and shortage of appropriate detectors.[19,34] In this study, we also carried out measurements to detect $^1O_2$ using an experimental setup like the one proposed by Boso *et al.* This method allows direct detection of the singlet oxygen generation during the first instants of the stimulation. The samples with MB, RB and C were excited with a laser diode (300 mW Laserland RGB laser module) at 660 nm (120 mW), 515 nm (50 mW) and 450 nm (130 mW), respectively, whereas R and P were irradiated at 405 nm (200 mW) (Laserland). The exposure time depended on the PS. A pair of converging lenses were used to conduct the beam to a dichroic mirror (DMLP900, Thorlabs). It does a double function, reflects the beam to the sample and transmits the infrared signal coming from the sample towards two filters. The first is a long-pass filter (1200 nm), and the second is a short-pass filter (1300 nm), (67-296 and 84-642, Edmund Optics), which guaranties only the detection of $^1O_2$. A lens concentrates the infrared radiation into an InGaAs commercial detector (918D-IG-OD1R, Newport) designed for low optical power measurements in the spectral range between 800 nm and 1650 nm. It is connected to a power meter (1918-R, Newport). It produces a power signal when infrared photons impinge on it. PS samples of 1 mL were placed in a 35 mm Petri dish and exposed to radiation for 5 min. The concentrations were 25 mM in all cases except for P, which was 1.42 μg/mL. MB, RB and P were dissolved in Milli-Q water, while C and R were mixed in dimethyl sulfoxide. Each one was measured by triplicate. The control sample was Milli-Q water.

3. Results

As a control experiment, we evaluated the survival percentages and CFU of *E. coli* exposed to light without PS: red (RL), green (GL), blue (BL) and UV-A radiation (see Fig. 6). As expected, there is no inhibition, except in the case of UV-A where a slight effect is observed probably due to the *E. coli* endogenous sensitizers.

Figure 7 shows the effect of photoinactivation in *E. coli* with different PS exposed to their corresponding wavelengths. The comparison is made by matching the number of photons absorbed by the PSs according to their chemical characteristics, which involved different concentrations (from 3.1 μg/mL to 82.3 μg/mL). Dark conditions, (PBS + PS) did not produce cell damage. In the photoinactivation experiments the combination of cationic MB + RL resulted in the greatest inactivation (3 $\log_{10}$) after 60 min of irradiation. Meanwhile, the action of anionic and neutral PS, RB + GL and R + UV-A produced a reduction of

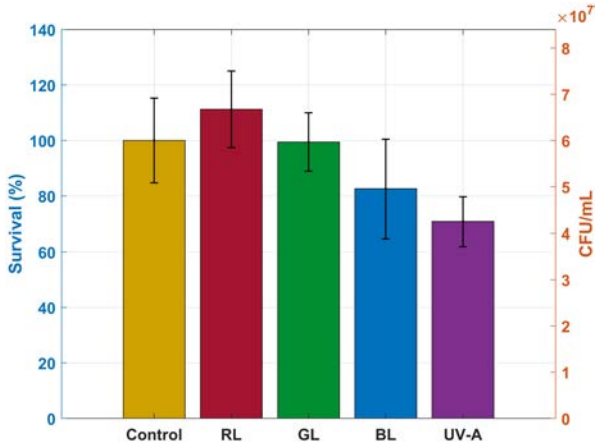

Fig. 6. Reduction of *E. coli* bacteria without PS exposed during 60 min: RL (660 nm), GL (515 nm), BL (450 nm) and UV-A radiation (375 nm). Laser diodes (300 mW RGB combined mixed white laser module mini stage lighting, Laserland) were used for irradiations of cultures with MB, RB and C. UV-A laser (Excelsior, Spectra-Physics) was used for irradiations of cultures with R and P. The same number of absorbed photons in all the cases was guaranteed using a circular neutral density filter (CVND15-B60C, Opto Science Inc.) and the dose was 95.27 J cm^{-2}. The data are shown in terms of survival percentages (left axis) and CFU/mL (right axis).

2.3 $\log_{10}$ and 1.7 $\log_{10}$ steps, respectively. In contrast, the result of P + UV-A was not as effective (< 1 $\log_{10}$), and C + BL did not produce any change. In this regard, it has been reported that C with BL is approximately 300 times more effective in Gram-positive (*S. aureus*) than in Gram-negative (*Salmonella typhimurium*) bacteria.[35] In that work, the samples were exposed in a medium with 8.8 ppm O_2. At 10 μM of C, the inactivation obtained after 40 min irradiation was comparable to this study: (< 1 $\log_{10}$) at 9.77 μM/mL and 60 min exposure.

When EDTA is added to the cultures in dark conditions, (PBS + EDTA), no change is observed (see Fig. 8). The addition of the PS, (PBS + EDTA + PS), showed an insignificant effect. However, when light was applied to the cultures, (PBS + EDTA + PS + Light), the reductions obtained in the viable counts were: MB, 4.7 $\log_{10}$; C, 3.3 $\log_{10}$; RB, 2.7 $\log_{10}$; R, 2.6 $\log_{10}$ and P, 2 $\log_{10}$.

In order to properly assess the effect produced on the PS by light, it is crucial to explore the production of ROS by fluorescence experiments. First, we measured $^1O_2$, the major cytotoxic agent generated

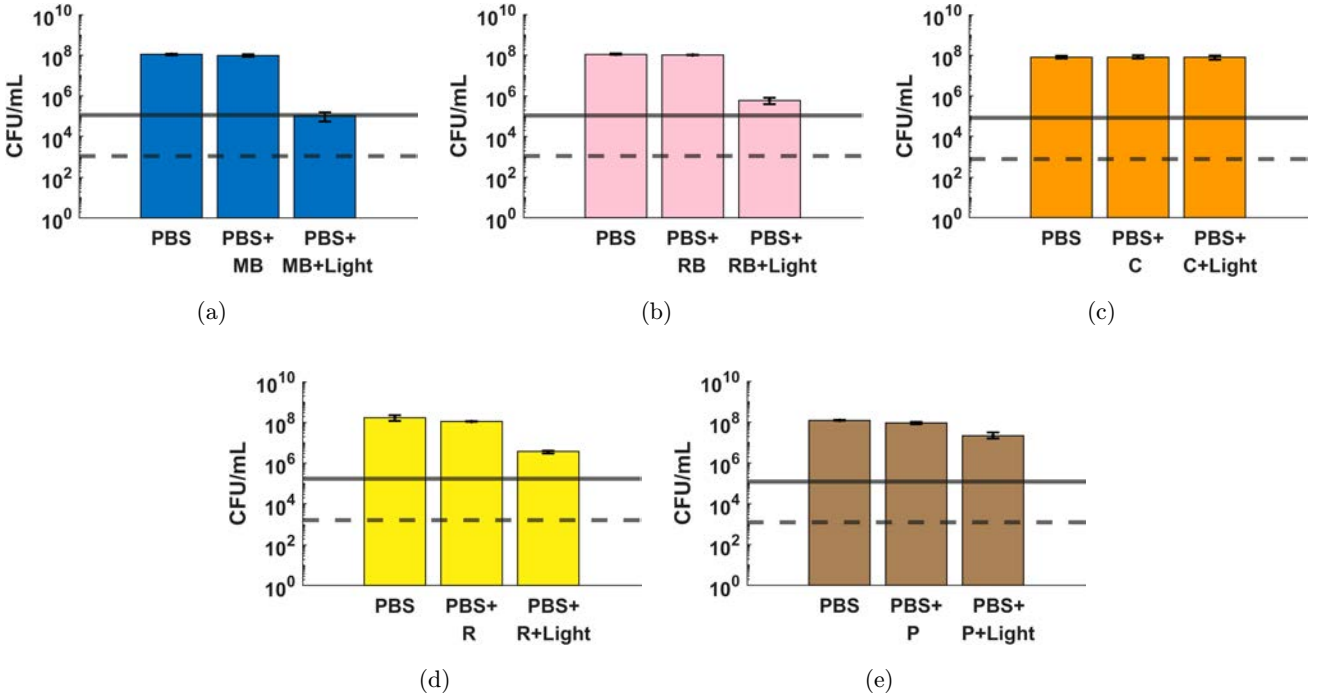

Fig. 7. Inactivation of *E. coli* bacteria exposed to five different PS (four commercial and one synthesized in the laboratory): (a) MB (12.5 μg/mL) at 660 nm, (b) RB (13.2 μg/mL) at 515 nm, (c) C (3.1 μg/mL) at 450 nm, (d) R (54.5 μg/mL) at 375 nm and (e) P (82.3 μg/mL) at 375 nm. The results are shown as CFU medians with 25% and 75% quartiles exhibited on a $\log_{10}$ scaled ordinate. Medians on or below the continuous and dashed lines indicate CFU diminutions of ≥ 3 $\log_{10}$ and ≥ 5 $\log_{10}$ steps, respectively, compared to the control (PBS). The cultures were exposed 60 min (95.27 J cm^{-2}), at 26.45 mW cm^{-2} irradiance. Abbreviations: PBS — phosphate-buffered saline; PBS + PS: PS in PBS (no light).

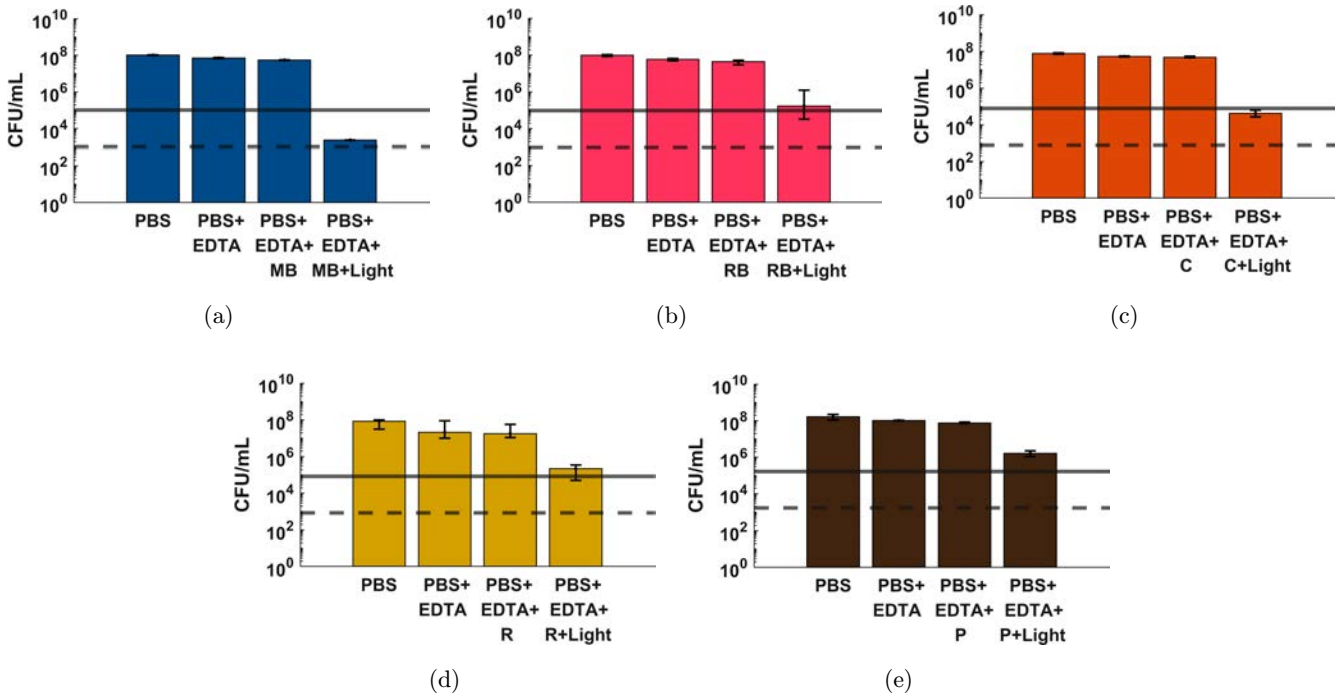

Fig. 8. Inactivation of *E. coli* bacteria exposed to five different PS (four commercial and one synthesized in the laboratory) and their combination with EDTA: (a) MB (12.5 μg/mL) at 660 nm, (b) RB (13.2 μg/mL) at 515 nm, (c) C (3.1 μg/mL) at 450 nm, (d) R (54.5 μg/mL) at 375 nm and (e) P (82.3 μg/mL) at 375 nm. The results are shown as CFU medians with 25% and 75% quartiles exhibited on a $\log_{10}$ scaled ordinate. Medians on or below the continuous and dashed lines indicate CFU diminutions of ≥ 3 $\log_{10}$ and ≥ 5 $\log_{10}$ steps, respectively, compared to the control (PBS). The cultures were exposed 60 min (95.27 J cm^{-2}), at 26.45 mW cm^{-2} irradiance. Abbreviations: PBS — phosphate-buffered saline; EDTA — chelant agent (ethylenediaminetetraacetic acid); PBS + PS: PS in PBS (no light); PBS + PS + EDTA: PS in PBS and EDTA (no light).

during PDI. In Fig. 9, we show the fluorescence emission spectra obtained from each case: PS, SOSG and a combination of both, before and after irradiation. The intrinsic fluorescence of each illuminated PS can observed. SOSG also emits fluorescence by itself, as reported by other authors.[36,37] In particular, the combinations R + SOSG and RB + SOSG show clearly that there is no chemical interaction between the two compounds before irradiation. In general, the green fluorescence intensity from SOSG-EP increases as the sample is irradiated. Moreover, the rate generation, matching the number of absorbed photons that every PS exhibits, occurs at different time scales. For instance, R needs short exposure times to active $^1O_2$ and produce similar fluorescence intensity than other PSs, and the changes in fluorescence are more evident for R. In contrast, using P requires longer exposures to produce similar fluorescence. These results are associated with the structure and properties of each PS. In particular, R and C are neutral molecules, however, R has a quantum yield (Φ_Δ) twelve times greater than C (around 0.6[29,33]), meaning that the first has a greater capacity to generate $^1O_2$ than the last. This is related to the rapid absorption of photons and the saturation exhibited by C (see Fig. 3), which explains why the production of $^1O_2$ during the irradiation occurs at shorter exposures than those for C. On the other hand, MB is a cationic and hydrophilic molecule, but it has a similar quantum yield to R,[29,30] requiring comparable irradiation times to produce similar fluorescence intensities.

Analogously, we detected hydroxyl radical and peroxynitrite generated from HPF by irradiation of the PS solution (see Fig. 10). MB, RB and R have the maximum fluorescence emission peaks at 682, 568 and 525 nm, respectively, with a negligible fluorescence at 515 nm, where HPF is significant. In general, it is observed that the combinations RB + SOSG, R + SOSG and P + SOSG undoubtedly show that there is no chemical interaction between the two compounds before irradiation. The fluorescence intensity increases as the samples are exposed to the wavelength of maximum absorbance of the PS. In the case of C and P, such generation is

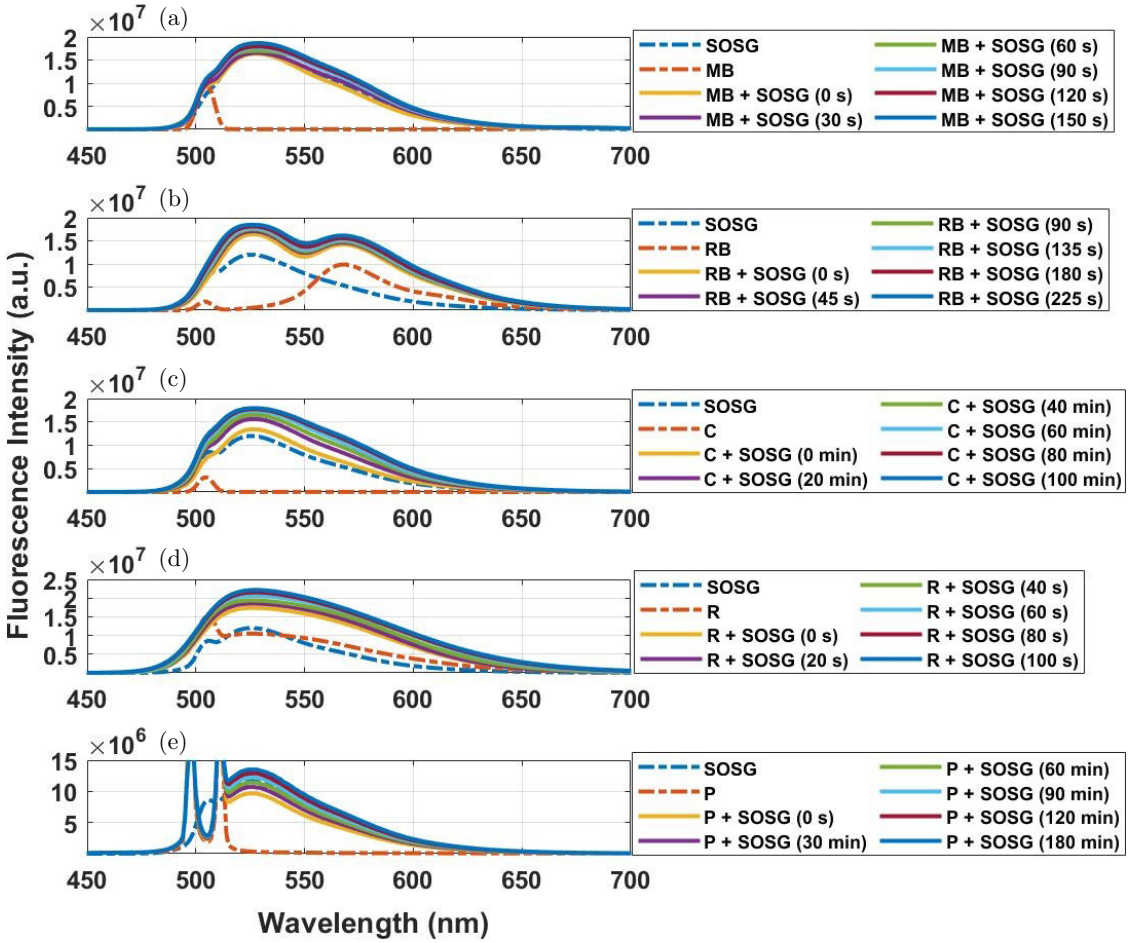

Fig. 9. Detection of $^1O_2$ in *E. coli* cultures incubated with five different PS: MB, RB, C, R and P, using SOSG. The fluorescence intensity was measured between 400 nm and 800 nm with excitation at 504 nm. SOSG was diluted in a mix of methanol and PBS buffer (4 μM). One part of this stock solution was combined with nine parts of the PS suspension: 19.8, 8.19, 4.52, 62, 37.4 μg/mL for MB, RB, C, R and P, respectively. Final concentration of the samples with PS and SOSG was 17.8, 7.37, 4.07, 55.8 and 33.7 μg/mL for the same PSs. Every sample was irradiated with the appropriate wavelength for different periods. SOSG detection was performed immediately after irradiation in five steps. Exposure time was fixed according to each PS and the equipment characteristics.

more notorious at the beginning of the irradiation procedure (30 min and 60 min), and the fluorescence slightly changes from 100 min. The opposite situation is observed for MB, where the greater production of ROS occurs between 120 s and 150 s.

To detect singlet oxygen, we also carried out a second measuring method using a solid-state detector (InGaAs). Figure 11 exhibits the power intensity in real time as the sample with PS is excited at the appropriate wavelength. We observe the immediate generation of $^1O_2$ as the signal continuously increases, reaching a maximum value in some cases due to a saturation in the power intensity, which occurs approximately after 300 s in all the cases, except for C (around 45 s), where the generation looks ephemeral, contrary to P.

4. Discussion

To ensure an efficient procedure in clinical practice based on PDI, it is crucial to compare the effects obtained by different wavelengths and PSs. However, the comparison process is not an easy task because the chemical properties of a given PS determine its extinction coefficient and the power of the light source determines the energy and fluence. A noteworthy method to compare different PDI practices was suggested by a research group,[22] which is based on matching the number of photons absorbed by the PS. The idea is of a great value because it is the number of photons absorbed that determines the production of ROS.

In this work, we carried out a comparative study of PDI in *E. coli* cultures considering the mentioned

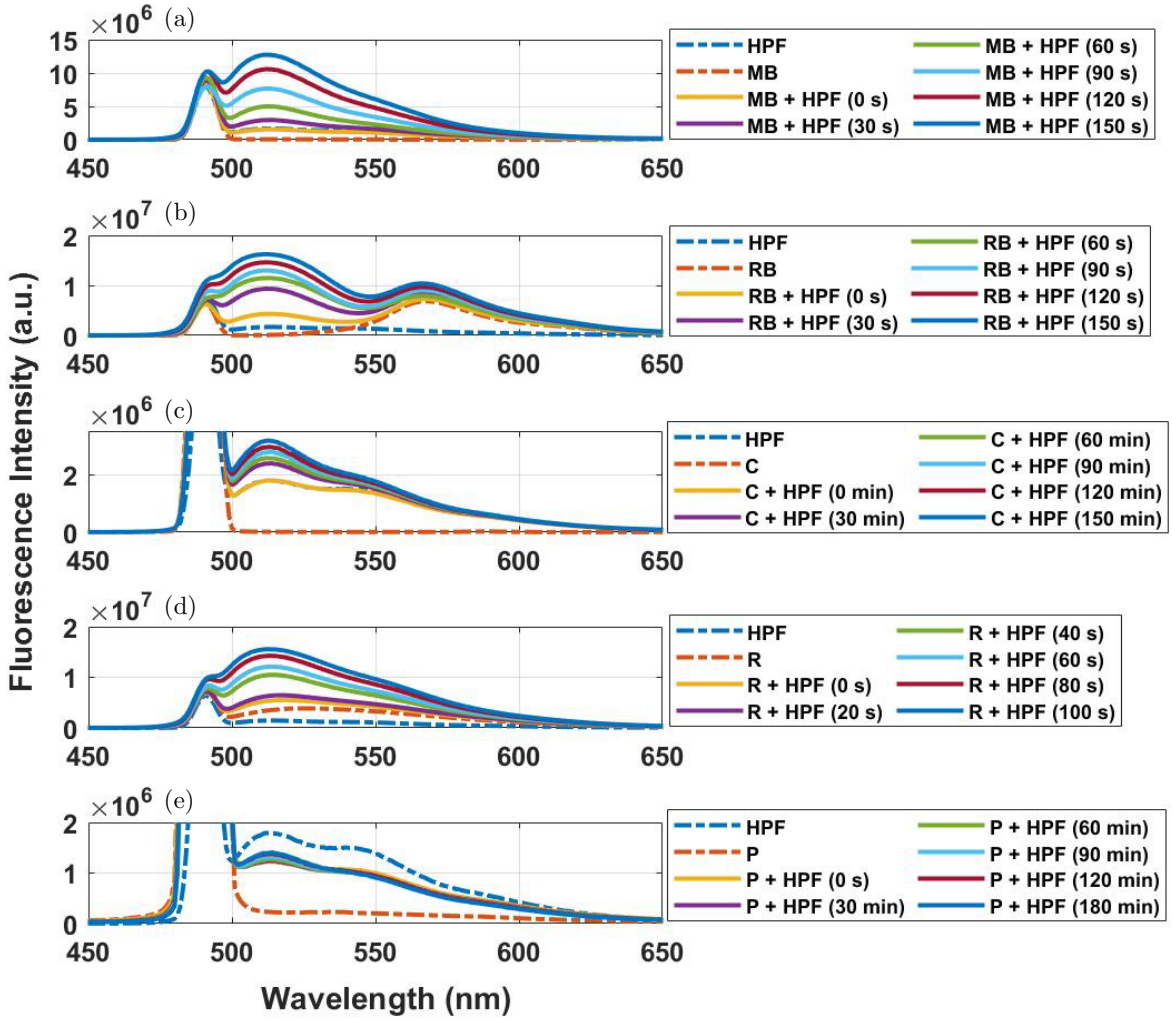

Fig. 10. Detection of $^{\cdot}$OH in *E. coli* cultures incubated with five different PS: MB, RB, C, R and P, using HPF. The fluorescence intensity was measured between 400 nm and 800 nm with excitation at 490 nm. HPF was diluted in a mix of methanol and PBS buffer (4 μM). One part of this stock solution was combined with nine parts of the PS suspension: 19.8, 8.19, 4.52, 62, 37.4 μg/mL for MB, RB, C, R and P, respectively. Final concentration of the samples with PS and HPF was 17.8, 7.37, 4.07, 55.8 and 33.7 μg/mL for the same PSs. Every sample was irradiated for different periods. HPF measurements were performed immediately after irradiation in five steps. Exposure time was fixed according to each PS and the equipment characteristics.

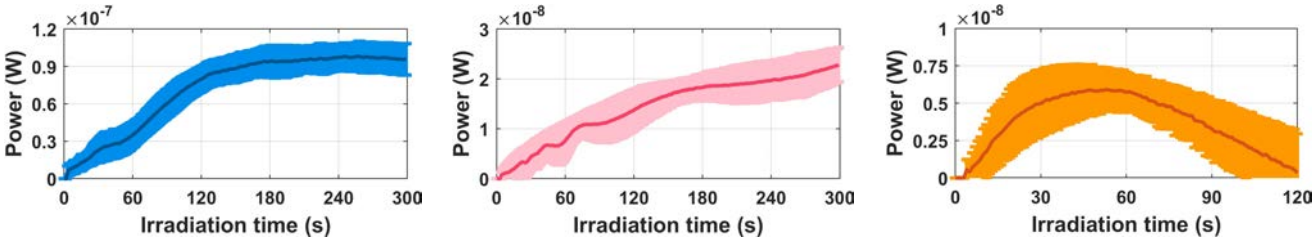

(a) (b) (c)

Fig. 11. Power measured when infrared photons from singlet oxygen impinge on the detector during exposure to visible (a)–(c) and UV-A radiation (d) and (e). Panel (e) corresponds to water response exposed to visible light (control). The detection is performed by commercial InGaAs detector that is connected to a power meter, which produces a signal when infrared photons arrive. The measurements were obtained every second for 5 min. The black line is the average, and the band is the dispersion of the data from three independent experiments. The large dispersion is inherent to the detection method.

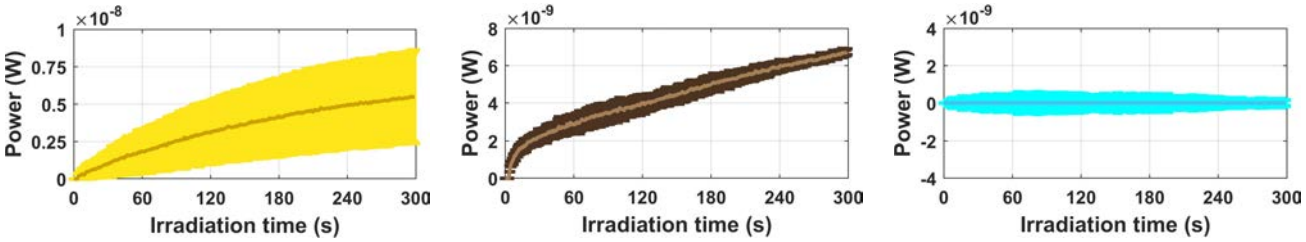

(d) (e) (f)

Fig. 11. (*Continued*)

idea,[22] with the following caveat: instead of a summatory in Eq. (1) we integrate in wavelength over the spectra range. We evaluated five PSs with different charge and water affinity. These were MB, RB, C, R and P, which was synthesized and characterized in our laboratory.[27]

Based on the response of C and P, we selected the specific number of absorbed photons per second as 8×10^{15} for the five PSs, considering the response of each one as a function of their concentration. The parameters associated to PS and light source, as well as the spectral radial power measured, were plugged in the proposed master equation (see Introduction).[22]

None of the five PSs used in this study showed bacterial toxicity in dark conditions. We found that the most efficient photoinactivation (3 $\log_{10}$) occurs using MB (39.1 μM) and exposed to RL at 95.27 J cm^{-2} for 60 min, see Fig. 7. This result could be explained because MB is a cationic and hydrophilic phenothiazinium dye that binds to both Gram-positive and Gram-negative bacteria.[29,33] Moreover, it exhibited the highest $^1O_2$ quantum yield compared to the other PSs in this study. It should be noted that other studies report higher efficacy than MB using other PS matching the absorbed photons. This involves energy doses of 3.6 J cm^{-2} and 30 J cm^{-2} and exposure periods of 600 s and 181 s, respectively.[22] Under these experimental conditions, MB can be considered as antibacterial (due to reduction of 3 $\log_{10}$ steps).[38]

With the chosen parameters, C and BL did not have reduction on CFU. It should be noted that the generation and saturation of $^1O_2$ is fastest in C than in any other PS (see Fig. 9) in accordance to Schneider *et al.*[39] that reported that C incubated in cultured cells rapidly degrades to other chemical species by autoxidation process. They claim that, although the effects of C have been analyzed using some general antioxidants, it is necessary to make more studies to rule out if these are not due to the degradation products of C. On the other hand, the potential of different solvents and carriers for C have been evaluated (at 1–25 μM) using antimicrobial photodynamic therapy with pharmaceutical purposes. The reason is that C exhibits a phototoxic effect depending on its concentration, polarity of molecular environment and light exposure time.[40] In this work, we used C with the lowest (almost null) cytotoxicity and the highest purity.

Treatment with P and UV-A exhibited similar results to those with C and BL (see Fig. 7), which is due to their poor ability to generate ROS. Because PLs in membranes are tightly packed and there is not much room for insertion of external intruders, large molecules are difficult to diffuse. Since the nanoparticles of P have a diameter between 90 nm and 180 nm,[27] the production of ROS is certainly outside the membrane. In the case of RB, it has been reported that extra and intracellular targets in *E. coli* are the cytoplasmic membrane and probably DNA[41] and it exits a lag time due to the LPS coat.

The addition of EDTA to the cultures improved the photoinactivation in all cases, notoriously in C (3.3 $\log_{10}$).

Previous studies in our laboratory using *E. coli* have shown that P behaves as a good PS. It exhibits a negative superficial charge (−31 mV), and the addition of EDTA improves its effect in cell cultures.[27] In this work, due to the chosen parameters for matching, it only produces 2 $\log_{10}$ of bacteria inactivation.

Fluorescence spectroscopy and a solid-state detector were used to evaluate the generation of ROS at different time scales. The second method allowed the detection of $^1O_2$ during the first instants of irradiation. We confirm that C is very photo-labile molecule, it easily degraded under light[42] and it is a

poor $^1O_2$ generator. Meanwhile, the production of singlet oxygen from P increases gradually and slowly. Contrary, MB rapidly augments and reaches saturation after around 2.5 min.

Normally, in photoinactivation experiments photobleaching could occur. However, since in our work we compared five PSs if photobleaching takes place, this is implicit in the results. We would like to remark that according to fluorescence measurements we did not see any decrement in the response of C and P after more than 100 min of irradiation. Therefore, photoinactivation for one hour was a good selection.

In the last years, there have been many works reporting the photoinactivation effect of PSs like those used in this study with different purposes, including clinical application. For instance, Svyatchenko *et al.* evaluated the antiviral photodynamic effect in Vero cells infected by SARS-CoV-2 in presence of MB and Radachlorin exposed to RL. The method showed an important antiviral activity by light microscopy after 3.5 h of infection cells.[43] Nima *et al.* applied C (5 mM) and EDTA (0.125%) against *Streptococcus mutans*. The authors achieved a complete inactivation of bacteria resulting in a promising method for dental tissue disinfection.[44] Their results coincide with ours in the sense that EDTA enhances the action of C. Nima *et al.* employed RB (160 μg/mL) and BL (12 J cm^{-2}) to annihilate several pathogens that cause periodontal infections obtaining log reductions above 2.[44] Rivas Aiello *et al.* enhanced the photoinactivation effect of R using pectin-coated gold nanoparticles on *S. aureus* and *P. aeruginosa*.[45]

Because the important problem of the antimicrobial resistance, new molecules are frequently introduced as PSs, or already used ones with novel strategies. To evaluate their inhibitory effect, it is necessary to compare their action with an already known molecule. In this context, it is crucial to emphasize that an appropriate method to carry out such comparison could be the one we discuss in this work.

5. Conclusions

We compared the effect of five different PSs in *E. coli* cultures, considering the same number of absorbed photons. Our findings reveal that MB excited with RL produces the highest inactivation (3 $\log_{10}$) and the addition of EDTA increases it to 4.7 $\log_{10}$. PDI efficacy between different PSs, that essentially depends on the extinction coefficient and light power, is usually highest for some PSs when their action is individually studied. However, when compared at the same conditions of absorbed photons, we see distinct effects. In other words, only this correct way to compare between different PSs give us the information about their efficacy. The results can be improved if the study is restricted to PS with similar absorption spectra increasing the number of absorbed photons, a project we will pursue in the future.

Conflict of Interest

The authors declare that there are no conflicts of interest relevant to this paper.

Acknowledgments

This work was supported by CONACyT, Mexico under Grant A1-S-8125 and Fideicomiso SEP-CINVESTAV (FIDSC2018/72). Daniel Ortega-Zambrano and Denisse Fuentes-López received a scholarship from CONACyT.

References

1. T. Dai, Y.-Y. Huang, M. R. Hamblin, "Photodynamic therapy for localized infections — State of the art," *Photodiagn. Photodyn. Ther.* **6**(3–4), 170–188 (2009).
2. M. Ahmad, A. U. Khan, "Global economic impact of antibiotic resistance: A review," *J. Glob. Antimicrob. Resist.* **19**, 313–316 (2019).
3. F. Cieplik, D. Deng, W. Crielaard, W. Buchalla, E. Hellwig, A. Al-Ahmad, T. Maisch, "Antimicrobial photodynamic therapy — What we know and what we don't," *Crit. Rev. Microbiol.* **44**(5), 571–589 (2018).
4. M. Wainwright, T. Maisch, S. Nonell, K. Plaetzer, A. Almeida, G. P. Tegos, M. R. Hamblin, "Photoantimicrobials — Are We afraid of the light?," *Lancet Infect. Dis.* **17**(2), e49–e55 (2017).
5. S. R. Norrby, C. E. Nord, R. Finch, "Lack of development of new antimicrobial drugs: A potential serious threat to public health," *Lancet Infect. Dis.* **5**(2), 115–119 (2005).
6. A. C. Rios, C. G. Moutinho, F. C. Pinto, F. S. Del Fiol, A. Jozala, M. V. Chaud, M. M. Vila, J. A. Teixeira, V. M. Balcão, "Alternatives to overcoming bacterial resistances: State-of-the-art," *Microbiol. Res.* **191**, 51–80 (2016).
7. E. Tacconelli, E. Carrara, A. Savoldi, S. Harbarth, M. Mendelson, D. L. Monnet, C. Pulcini, G. Kahlmeter,

J. Kluytmans, Y. Carmeli, "Discovery, research, and development of new antibiotics: The WHO priority list of antibiotic-resistant bacteria and tuberculosis," *Lancet Infect. Dis.* **18**(3), 318–327 (2018).
8. U. Theuretzbacher, K. Outterson, A. Engel, A. Karlén, "The global preclinical antibacterial pipeline," *Nat. Rev. Microbiol.* **18**(5), 275–285 (2020).
9. F. F. Sperandio, Y.-Y. Huang, M. R. Hamblin, "Antimicrobial photodynamic therapy to kill Gram-negative bacteria," *Recent Pat. Anti-Infect. Drug Discov.* **8**(2), 108–120 (2013).
10. R. E. Hancock, "Alterations in outer membrane permeability," *Annu. Rev. Microbiol.* **38**(1), 237–264 (1984).
11. L. H. Z. Malik, B. Ehrenberg, Y. Nitzan, *Photodynamic Therapy* (CRC Press, New York, NY, 1992).
12. E. Alves, N. Santos, T. Melo, E. Maciel, M. L. Dória, M. A. Faustino, J. P. Tomé, M. G. Neves, J. A. Cavaleiro, Ø. Cunha, "Photodynamic oxidation of *Escherichia coli* membrane phospholipids: New insights based on lipidomics," *Rapid Commun. Mass Spectrom.* **27**(23), 2717–2728 (2013).
13. M. E. Forman, M. H. Fletcher, M. C. Jennings, S. M. Duggan, K. P. Minbiole, W. M. Wuest, "Structure–resistance relationships: Interrogating antiseptic resistance in bacteria with multicationic quaternary ammonium dyes," *ChemMedChem* **11** (9), 958–962 (2016).
14. F. Cieplik, N. S. Jakubovics, W. Buchalla, T. Maisch, E. Hellwig, A. Al-Ahmad, "Resistance toward chlorhexidine in oral bacteria — Is there cause for concern?," *Front. Microbiol.* **10**, 587 (2019).
15. H. Venter, M. L. Henningsen, S. L. Begg, "Antimicrobial resistance in healthcare, agriculture and the environment: The biochemistry behind the headlines," *Essays Biochem.* **61**(1), 1–10 (2017).
16. L. Benov, "Photodynamic therapy: Current status and future directions," *Med. Princ. Pract.* **24** (Suppl. 1), 14–28 (2015).
17. L. Costa, M. A. F. Faustino, M. G. P. Neves, Ø. Cunha, A. Almeida, "Photodynamic inactivation of mammalian viruses and bacteriophages," *Viruses* **4**(7), 1034–1074 (2012).
18. H. Abrahamse, M. R. Hamblin, "New photosensitizers for photodynamic therapy," *Biochem. J.* **473**(4), 347–364 (2016).
19. P. R. Ogilby, "Singlet oxygen: There is indeed something new under the sun," *Chem. Soc. Rev.* **39** (8), 3181–3209 (2010).
20. A. Preuss, L. Zeugner, S. Hackbarth, M. Faustino, M. Neves, J. Cavaleiro, B. Roeder, "Photoinactivation of *Escherichia coli* (SURE 2) without intracellular uptake of the photosensitizer," *J. Appl. Microbiol.* **114**(1), 36–43 (2013).
21. P. Acedo, J. Stockert, M. Cañete, A. Villanueva, "Two combined photosensitizers: A goal for more effective photodynamic therapy of cancer," *Cell Death Dis.* **5**(3), e1122 (2014).
22. F. Cieplik, A. Pummer, J. Regensburger, K.-A. Hiller, A. Späth, L. Tabenski, W. Buchalla, T. Maisch, "The impact of absorbed photons on antimicrobial photodynamic efficacy," *Front. Microbiol.* **6**, 706 (2015).
23. F. Cieplik, A. Pummer, C. Leibl, J. Regensburger, G. Schmalz, W. Buchalla, K.-A. Hiller, T. Maisch, "Photodynamic inactivation of root canal bacteria by light activation through human dental hard and simulated surrounding tissue," *Front. Microbiol.* **7**, 929 (2016).
24. T. D. Le, P. Phasupan, L. T. Nguyen, "Antimicrobial photodynamic efficacy of selected natural photosensitizers against food pathogens: Impacts and interrelationship of process parameters," *Photodiagn. Photodyn. Ther.* **32**, 102024 (2020).
25. P. Phasupan, T. D. Le, L. T. Nguyen, "Assessing the photodynamic efficacy of different photosensitizer-light treatments against foodborne bacteria based on the number of absorbed photons," *J. Photochem. Photobiol. B* **221**, 112249 (2021).
26. D. Muehler, E. Brandl, K.-A. Hiller, F. Cieplik, T. Maisch, "Membrane damage as mechanism of photodynamic inactivation using methylene blue and TMPyP in *Escherichia coli* and *Staphylococcus aureus*," *Photochem. Photobiol. Sci.* **21**, 209–220 (2022).
27. D. Fuentes-López, D. Ortega-Zambrano, M. A. Fernández-Herrera, H. Mercado-Uribe, "The growth of *Escherichia coli* cultures under the influence of pheomelanin nanoparticles and a chelant agent in the presence of light," *PLoS One* **17**(3), e0265277 (2022).
28. M. Peleg, M. G. Corradini, "Microbial growth curves: What the models tell us and what they cannot," *Crit. Rev. Food Sci. Nutr.* **51**(10), 917–945 (2011).
29. L. Sobotta, P. Skupin-Mrugalska, J. Piskorz, J. Mielcarek, "Non-porphyrinoid photosensitizers mediated photodynamic inactivation against bacteria," *Dyes Pigments* **163**, 337–355 (2019).
30. L. V. Lutkus, S. S. Rickenbach, T. M. McCormick, "Singlet oxygen quantum yields determined by oxygen consumption," *J. Photochem. Photobiol. A* **378**, 131–135 (2019).
31. L. C. P. Gonçalves, "Photophysical properties and therapeutic use of natural photosensitizers," *J. Photochem. Photobiol.* **7**, 100052 (2021).
32. M. Condat, P.-E. Mazeran, J.-P. Malval, J. Lalevée, F. Morlet-Savary, E. Renard, V. Langlois, S. A. Andalloussi, D.-L. Versace, "Photoinduced curcumin

derivative-coatings with antibacterial properties," *RSC Adv.* **5**(104), 85214–85224 (2015).
33. J. Baier, T. Maisch, M. Maier, E. Engel, M. Landthaler, W. Bäumler, "Singlet oxygen generation by UVA light exposure of endogenous photosensitizers," *Biophys. J.* **91**(4), 1452–1459 (2006).
34. G. Boso, D. Ke, B. Korzh, J. Bouilloux, N. Lange, H. Zbinden, "Time-resolved singlet-oxygen luminescence detection with an efficient and practical semiconductor single-photon detector," *Biomed. Opt. Express* **7**(1), 211–224 (2016).
35. T. A. Dahl, W. M. McGowan, M. A. Shand, V. S. Srinivasan, "Photokilling of bacteria by the natural dye curcumin," *Archiv. Microbiol.* **151**(2), 183–185 (1989).
36. X. Ragàs, A. Jiménez-Banzo, D. Sánchez-García, X. Batllori, S. Nonell, "Singlet oxygen photosensitisation by the fluorescent probe Singlet Oxygen Sensor Green®," *Chem. Commun. (20)*, 2920–2922 (2009).
37. S. Nonell, S. E. Braslavsky, "Time-resolved singlet oxygen detection," *Methods Enzymol.* **319**, 37–49 (2000).
38. J. M. Boyce, D. Pittet, "Guideline for hand hygiene in health-care settings: Recommendations of the Healthcare Infection Control Practices Advisory Committee and the HICPAC/SHEA/APIC/IDSA Hand Hygiene Task Force," *Infect. Control Hosp. Epidemiol.* **23**(S12), S3–S40 (2002).
39. C. Schneider, O. N. Gordon, R. L. Edwards, P. B. Luis, "Degradation of curcumin: From mechanism to biological implications," *J. Agric. Food Chem.* **63** (35), 7606–7614 (2015).
40. T. Haukvik, E. Bruzell, S. Kristensen, H. Tønnesen, "Photokilling of bacteria by curcumin in selected polyethylene glycol 400 (PEG 400) preparations. Studies on curcumin and curcuminoids, XLI," *Pharmazie* **65**(8), 600–606 (2010).
41. Y. Liu, R. Qin, S. A. Zaat, E. Breukink, M. Heger, "Antibacterial photodynamic therapy: Overview of a promising approach to fight antibiotic-resistant bacterial infections," *J. Clin. Trans. Res.* **1**(3), 140 (2015).
42. M. Heger, R. F. van Golen, M. Broekgaarden, M. C. Michel, "The molecular basis for the pharmacokinetics and pharmacodynamics of curcumin and its metabolites in relation to cancer," *Pharmacol. Rev.* **66**(1), 222–307 (2014).
43. V. A. Svyatchenko, S. D. Nikonov, A. P. Mayorov, M. L. Gelfond, V. B. Loktev, "Antiviral photodynamic therapy: Inactivation and inhibition of SARS-CoV-2 in vitro using methylene blue and Radachlorin," *Photodiagn. Photodyn. Ther.* **33**, 102112 (2021).
44. G. Nima, J. Soto-Montero, L. A. Alves, R. O. Mattos-Graner, M. Giannini, "Photodynamic inactivation of *Streptococcus mutans* by curcumin in combination with EDTA," *Dent. Mater.* **37**(1), e1–e14 (2021).
45. M. B. Rivas Aiello, F. Ghilini, J. E. Martinez Porcel, L. Giovanetti, P. L. Schilardi, D. O. Mártire, "Riboflavin-mediated photooxidation of gold nanoparticles and its effect on the inactivation of bacteria," *Langmuir* **36**(28), 8272–8281 (2020).